

Chromium isotope fractionation factors for reduction of Cr(VI) by aqueous Fe(II) and organic molecules

Jacquelyn W. Kitchen^a, Thomas M. Johnson^{a,*}, Thomas D. Bullen^b,
Jianming Zhu^c, Amanda Raddatz^a

^a Department of Geology, University of Illinois at Urbana-Champaign, Urbana, IL 61801, USA

^b Water Resources Division, US Geological Survey, Menlo Park, CA 94025, USA

^c The State Key Lab of Environmental Geochemistry, Institute of Geochemistry,
Chinese Academy of Sciences, Guiyang 550002, China

Received 7 September 2011; accepted in revised form 23 April 2012; available online 30 April 2012

Abstract

Chromium stable isotope ratios are useful as indicators of Cr redox reactions and Cr sources in both modern and ancient geochemical systems. Correct interpretation of Cr isotope data requires a quantitative understanding of isotopic fractionation by various processes, the most important of which is reduction of Cr(VI) to Cr(III). We determined the magnitude of isotopic fractionation, for the $^{53}\text{Cr}/^{52}\text{Cr}$ ratio, induced by abiotic, dark reduction of Cr(VI) by aqueous Fe(II) and a few organic substances. The isotopic fractionation for reduction by dissolved Fe(II), expressed as ϵ ($\approx \delta^{53}\text{Cr}_{\text{product flux}} - \delta^{53}\text{Cr}_{\text{reactant}}$) is $-4.20 \pm 0.11\%$ from pH = 4.0 to 5.3. Lesser fractionation was observed in preliminary experiments with very rapid reaction; we attribute this to transient heterogeneity and diffusive limitation of the reaction as reactants were mixed. This phenomenon is a general problem with batch isotopic fractionation experiments, if significant reaction occurs before mixing of reactants is complete. $\epsilon = -3.11 \pm 0.11\%$ for reduction by three organic reductants (a humic acid at pH = 4.5 and 5.0, a fulvic acid at pH = 5.0, and mandelic acid catalyzed by goethite or $\gamma\text{-Al}_2\text{O}_3$ at pH = 4.0).

© 2012 Elsevier Ltd. All rights reserved.

1. INTRODUCTION

The geochemistry of chromium depends strongly on redox reactions. Cr occurs in natural aqueous systems as Cr(VI) (+6 valence) and/or Cr(III) (+3 valence) (Ball and Nordstrom, 1998). Stable under oxidizing conditions, Cr(VI) forms the soluble, mobile chromate (CrO_4^{2-}), dichromate ($\text{Cr}_2\text{O}_7^{2-}$), and hydrochromate (HCrO_4^-) anions, with relative abundances depending on pH and Cr(VI) concentration. Cr(III) is stable under reducing conditions found in many sediments, soils and aquifers; it is sparingly soluble at circum-neutral pH, adsorbs strongly onto solid

surfaces, and is largely immobile. Cr(VI) is carcinogenic and otherwise toxic, whereas Cr(III) toxicity is relatively minor (US Department of Health, 2000). Reduction of Cr(VI) to Cr(III) can occur via microbial action (Lovley, 1993) or abiotic reactions (Palmer and Wittbrodt, 1991).

Many Cr-related geochemical questions focus on its redox shifts. Contamination of soil and water with Cr(VI) is common as a result of industrial activities (Proctor et al., 2000) or ultramafic rock weathering (e.g., Izbicki et al., 2008; Oze et al., 2007). Reduction of dissolved Cr(VI) to Cr(III) occurs naturally in some groundwater systems, rendering the Cr immobile and less toxic (Palmer and Puls, 1994). Artificial remediation can be carried out through biologically or abiotically induced reduction (Blowes et al., 2000; Faybishenko et al., 2008; Fruchter, 2002). Redox reactions play a role in the cycling of Cr in modern oceans and lakes (Johnson et al., 1992; Pettine, 2000). The strong redox sensitivity of Cr has also led to its

* Corresponding author. Address: Department of Geology, MC-102, 208 Natural History Bldg., University of Illinois at Urbana-Champaign, Urbana, IL 61801, USA. Tel.: +1 217 244 2002; fax: +1 217 244 4996.

E-mail address: tmjohnsn@illinois.edu (T.M. Johnson).

development as an indicator of paleo-redox conditions (Frei et al., 2009).

Recently, Cr stable isotope ($^{53}\text{Cr}/^{52}\text{Cr}$) variations have been developed as a new indicator of Cr sources and redox reactions (Johnson and Bullen, 2004). Isotopic fractionation induced by a chemical reaction can be quantified using a fractionation factor, α :

$$\alpha = \frac{(^{53}\text{Cr}/^{52}\text{Cr})_{\text{product flux}}}{(^{53}\text{Cr}/^{52}\text{Cr})_{\text{reactant}}} \quad (1)$$

Measured $^{53}\text{Cr}/^{52}\text{Cr}$ ratios are reported as relative deviations, in parts per thousand (per mil or ‰), from SRM 979 (a certified isotopic reference material distributed by NIST):

$$\delta^{53}\text{Cr} = \left[\frac{(^{53}\text{Cr}/^{52}\text{Cr})_{\text{measured}}}{(^{53}\text{Cr}/^{52}\text{Cr})_{\text{standard}}} - 1 \right] \times 1000\text{‰} \quad (2)$$

Similarly, a fractionation factor can be expressed using ϵ notation:

$$\epsilon = (\alpha - 1) \times 1000\text{‰} \quad (3)$$

This representation of the fractionation factor is convenient, as ϵ is very close to the difference in $\delta^{53}\text{Cr}$ between the reaction product flux and the Cr(VI) reactant:

$$\epsilon \approx \delta^{53}\text{Cr}_{\text{product flux}} - \delta^{53}\text{Cr}_{\text{reactant}} \quad (4)$$

Laboratory experiments have revealed that Cr(VI) reduction, like that of the other oxoanions nitrate, sulfate, perchlorate, and selenate, involves an enrichment of lighter isotopes in the products. The isotopic fractionation factor varies in magnitude, depending on reaction mechanism and other variables such as microbial reduction rate. Ellis et al. (2002) found $\epsilon = -3.4 \pm 0.1\text{‰}$ for abiotic reduction by magnetite and suspensions of two organic material-rich sediments. Sikora et al. (2008) studied Cr isotope fractionation during Cr(VI) reduction by the bacterium *Shewanella Oneidensis MR-1*. They found ϵ values close to -4.1‰ for several experiments with low electron donor concentrations (100 μM or less), and $\epsilon = -1.8 \pm 0.2\text{‰}$ for one experiment with much more electron donor (10 mM). Berna et al. (2010) determined ϵ values of -3.07‰ and -2.38‰ for two incubated sediments from a contaminated site. Zink et al. (2010) reported $\epsilon = -3.5$ and -5.0‰ for reduction by H_2O_2 under highly acidic and circum-neutral conditions, respectively. Experiments by Døssing et al. (2011) indicated $\epsilon = -3.0$ to -4.4‰ for reduction by aqueous Fe(II) at circum-neutral pH, and -1.5‰ for simultaneous reduction by dissolved Fe(II) and Fe(II) + Fe(III) “green rust.” Basu and Johnson (2012) reported $\epsilon = -3.91\text{‰}$ for reduction by Fe(II)-doped goethite, -2.11‰ for FeS, -2.65‰ for green rust, -2.67‰ for siderite (FeCO_3), and -3.18‰ for artificially reduced sediments from a permeable reactive barrier. These kinetically controlled isotopic shifts are smaller than equilibrium isotope fractionations: Wang and Johnson (2011) reported $\delta^{53}\text{Cr}(\text{VI}) - \delta^{53}\text{Cr}(\text{III}) = 4.9\text{‰}$ for isotopic equilibrium in an experiment containing 0.2 M Cr(VI) + 0.2 M Cr(III) at 60 °C, whereas Schauble et al. (2004) reported a theoretical estimate of 6–7‰ for Cr(VI)–Cr(III) equilibrium at 25 °C.

Several studies have used $\delta^{53}\text{Cr}$ measurements as a means of detecting redox reactions in various systems

and/or tracing sources of Cr(VI) in the environment. Because Cr(VI) reduction consumes lighter isotopes at a greater rate than heavier isotopes, elevated $\delta^{53}\text{Cr}$ values in groundwater Cr(VI) can provide evidence for the occurrence of Cr(VI) reduction. Izbicki et al. (2008, 2012) traced Cr sources and Cr(VI) reduction in groundwater of the Mojave desert, USA. Berna et al. (2010), Raddatz et al. (2010), Gao et al. (2010), and Wanner et al. (2012) used $\delta^{53}\text{Cr}$ data to provide evidence for Cr(VI) reduction in anthropogenic contaminant plumes.

$\delta^{53}\text{Cr}$ data from ancient rocks are emerging as potentially powerful indicators of paleo-redox conditions. Frei et al. (2009) found systematic $\delta^{53}\text{Cr}$ shifts in a series of banded iron formation samples from the 3.0 to 0.5 Ga time period, and argued that $\delta^{53}\text{Cr}$ data provide new insights to better constrain the nature and timing of paleo-redox changes.

In this study, we determined isotopic fractionation factors for homogeneous Cr(VI) reduction by aqueous Fe(II) and certain organic molecules. Aqueous Fe(II) is a key player in Cr geochemistry, as it readily reduces Cr(VI) (Buerge and Hug, 1997; Sedlak and Chan, 1997; Pettine et al., 1998), and occurs commonly in aquifers and other reducing waters on earth. Early in earth history, the oceans were Fe(II)-rich and thus Fe(II)-driven Cr reduction plays an important role in interpretations of Cr isotope data in paleoredox studies (Frei et al., 2009). Døssing et al. (2011) have already reported Cr isotope fractionation factors for homogeneous Cr(VI) reduction by aqueous Fe(II) at pH = 7. Here, we report results from a series of experiments determining the isotopic fractionation for this reaction over a range of pH, with special attention paid to avoiding potential complexity related to diffusion-limited reaction when Fe(II)–Cr(VI) interaction is very rapid.

Cr(VI) is readily reduced by many dissolved organic species (Elovitz and Fish, 1994; Deng and Stone, 1996; Wittbrodt and Palmer, 1996). The reaction rates are generally not as rapid as those observed with Fe(II) reduction, but organic reductants are common in natural waters and could be important Cr(VI)-reducers in cases where Fe(II) is absent. We determined isotopic fractionation factors for Cr(VI) reduction by two well-characterized natural humic substances. Because Cr(VI) reduction rates may be enhanced by catalysis on oxide surfaces, we also performed experiments with mandelic acid as the reductant, and goethite and $\gamma\text{-Al}_2\text{O}_3$ as catalysts.

2. MATERIALS AND METHODS

All solutions were prepared with 18 M Ω -cm deionized water. Temperature was maintained at 25 ± 3 °C. Experimental solutions contacted only sterilized materials to ensure microbial reactions did not occur, especially in the experiments with humic substances. All experiments were performed under anoxic conditions in pre-cleaned glass bottles, wrapped in aluminum foil to prevent photochemical reactions. The experimental media were placed in the bottles, autoclaved and sealed with Teflon-silicone or butyl rubber septa, cooled to room temperature, and sparged for 35 min with ultra-high purity N_2 gas to remove O_2 . Samples

were withdrawn using needles and syringes, with N_2 injected to replace withdrawn volumes. Some samples were stored for up to two weeks before processing for isotopic measurements. In those cases, Cr(VI) concentrations were re-measured after storage on a subset of the samples to confirm that reduction did not occur during storage.

2.1. Reduction experiments: dissolved Fe(II)

Cr(VI) reduction by dissolved Fe(II) was carried out using methods similar to the kinetic rate experiments reported by *Buerge and Hug (1997)*. Procedures were designed to avoid extremely rapid reaction rates, which can cause isotopic heterogeneity and lead to incorrect results (see Section 4). The rate of Cr(VI) reduction is a nearly linear function of OH^- concentration in the pH = 4–7 range (*Buerge and Hug, 1997*). Reactions were very rapid and difficult to control at pH > 5.5. Because the Cr(VI) reduction rate is proportional to Fe(II) concentration (*Buerge and Hug, 1997*), it was minimized to reduced reaction rates, and this in turn required low Cr concentrations. Solutions consisted of a background electrolyte solution of 0.01 M NaCl, with a pH buffer consisting of 1.0 mM sodium acetate (CH_3COOH ; used at pH 4.0, 4.5, and 5.0 and 5.3), or 1.0 mM 2-morpholinoethanesulfonic acid monohydrate (MES; $C_6H_{13}NO_4S$) (pH 6). Oxygen-free Fe(II) and Cr(VI) reagent solutions were made from $Fe(II)SO_4 \cdot 7H_2O$ and $K_2Cr_2O_7$, respectively. The pH of the Fe(II) stock solution was 3.5.

For each experiment, 100 mL of Cr(VI)-bearing buffer solution was placed in a 100 mL capacity glass septum bottle. Initial Cr(VI) concentrations were between 20 and 22 μM . Fe(II) was injected stepwise, with each step reducing a fraction of the Cr(VI) and oxidizing the Fe(II) completely. In preliminary experiments conducted at pH = 4.0, 5.0, and 6.0, the concentration of the added Fe(II) solution was 10 mM and the experimental solutions were shaken as quickly as possible, within about one minute, after injection.

Because the experiments at pH = 5.0 and 6.0 appeared to have suffered from fast reaction rates and potential heterogeneity problems (see Section 4), a second set of experiments, at pH = 4.5, 5.0, and 5.3 was designed more carefully, to prevent persistence of local zones of high Fe(II) concentrations and rapid reaction immediately after injection. The injected Fe(II) solution's concentration was reduced to 1 mM, and the volume injected was increased so that the mass of Fe(II) injected was about the same as in the preliminary experiments. Also, a stirring bar was used to vigorously stir the experimental solution as the Fe(II) was injected. Prior to the final experiments, this newer procedure was used in reduction rate tests conducted at pH 5.0 and 5.3 to confirm that reduction rates were slow enough so that thorough homogenization of the added Fe(II) could be achieved before substantial reduction occurred. In each rate test, Fe(II) was added to a solution containing 20 μM Cr(VI) in order to obtain 60 μM Fe(II) initially. The concentration of Fe(II) was measured over time to determine the reaction rate.

In the isotopic fractionation experiments, each stepwise Fe(II) addition initially brought the experimental solution's Fe(II) concentration to between 5 and 20 μM Fe(II). The volume added was a significant fraction of the total solution volume and caused slight dilution of the Cr(VI); volumes were carefully monitored and concentrations were later corrected accordingly. After Fe(II) addition, solutions were allowed to react for 24 h prior to sampling to ensure all Fe(II) was consumed and there was no potential for further reaction during sample storage. Cr(VI) loss matched that predicted from reaction stoichiometry (3 mol Fe(II) per mole Cr(VI) reduced) within the uncertainty of the injected volume (about $\pm 10\%$). After each reduction step was complete, samples were collected and filtered (0.45 μm). A yellowish color was observed on the filters, indicating the presence of a small quantity of an Fe(III)-oxyhydroxide precipitate. The mass of precipitate was very small; it was not visible in the experimental solution except toward the end of each experiment, when a slight yellowish color was observed. Calculations using the thermodynamic data of *Refait and Génin (1994)* indicated that Fe(II) + Fe(III) "green rust" phases were unstable under the experimental conditions. After each sample was taken, Cr(VI) concentrations were measured immediately, and samples were stored at 4 °C prior to preparation for isotopic analysis. Control experiments without added Fe(II) showed no significant reduction of Cr(VI) by the buffer solutions.

2.2. Reduction experiments: humic substances

Experiments were based on the kinetic studies of *Wittbrodt and Palmer (1996)*. Soluble humic substances were obtained from the International Humic Substances Society (IHSS) collection: Elliott Soil Fulvic Acid Standard II (2S102F) and Waskish Peat Humic Acid Reference (1R107H). In contrast to the Fe(II) experiments, where steps were taken to reduce reaction rates, humic substance reduction experiments were conducted to maximize reaction rates, which are quite slow and could lead to experiment durations of several months. Reduction rate increases with decreasing pH, so experiments were conducted at pH = 4.5 or 5.0 in order to complete the experiments within a few weeks time.

Each humic substance was dissolved in deionized water to create a 100 mg/L solution. The pH was adjusted to the desired value and the solution was equilibrated for 24 h before filtering 60 mL aliquots into 100 mL glass serum bottles. A $CaCl_2$ background electrolyte was added to attain an ionic strength of 0.1 M. Each bottle was autoclaved, sealed with a butyl rubber stopper, covered with aluminum foil, and cooled to room temperature before injecting Cr(VI) to attain an initial concentration of $21 \pm 0.5 \mu M$. Samples were withdrawn periodically as reduction proceeded, and concentrations were measured immediately. To stop the reactions and extract Cr(VI) for isotopic analysis without further reduction, sample preparation was begun within 20 min of sampling.

2.3. Surface-catalyzed reduction by an organic reductant

Experiments with surface-catalyzed reduction by mandelic acid followed the reaction rate investigation of [Deng and Stone \(1996\)](#). Mandelic acid ($C_8H_8O_3$) was chosen as a model alpha-hydroxyl carboxylic acid reductant. Solutions were buffered at pH 4.0 (5.0 mM sodium acetate buffer) to achieve reaction rates sufficient to complete the experiments in a few weeks' time. 0.1 M $NaClO_4$ was used as a supporting electrolyte, and two catalysts were used. The first was $\gamma-Al_2O_3$ (1.0 g/L; Degussa Corp) with a BET surface area of $96\text{ m}^2/\text{g}$, and point of zero charge at $pH = 8.9$. The second was Goethite (0.2 g/L; Bayferrox 910, Standard 86 obtained from Bayer AG) with a BET surface of $17.5\text{ m}^2/\text{g}$, and point of zero charge at $pH = 7.5\text{--}7.8$.

Experiments containing sorbents, Cr(VI), buffer, and supporting electrolyte were prepared in 1 L bottles. Solids were kept suspended by shaking on a rotary shaker table. Cr(VI) was allowed to equilibrate with sorbents for 24 h before reductant was added. Mandelic acid was injected to start the experiment with a concentration of $200\text{ }\mu\text{M}$. Samples were filtered ($0.45\text{ }\mu\text{m}$) to stop the reaction, and concentrations were measured immediately. Samples were stored at $4\text{ }^\circ\text{C}$ prior to preparation for isotopic analysis.

2.4. Analytical methods

Cr(VI) concentrations were measured within 5 min of sampling using EPA method 7196A. A diphenylcarbazide (DPC) indicator was added to acidified samples and visible light absorbance at 540 nm was measured using a Thermo Genesys 20 spectrophotometer. Reproducibility, determined by analyzing one out of every 5 samples in duplicate, was $\pm 4\%$ (2σ). Fe(II) concentrations were measured using the ferrozine colorimetric method ([Viollier et al., 2000](#)).

Cr(VI) was extracted from sample solutions and separated from dissolved Cr(III) and other solutes prior to isotopic analysis, following the method of [Ellis et al. \(2002\)](#). Solutions were processed within two weeks of sampling. Cr(VI)–Cr(III) isotopic exchange is known to be very slow ([Zink et al., 2010](#)), and should not have altered the isotopic compositions over that time period. High-purity quartz-distilled HCl was used for all steps. After extraction of samples from the bottles and filtration ($0.45\text{ }\mu\text{m}$) of the samples, a double isotope spike solution comprised of $^{54}\text{Cr} + ^{50}\text{Cr}$ in Cr(VI) form was added to aliquots of the filtered sample containing 1000–1500 ng Cr(VI). The double spike is used to correct for instrumental mass bias that occurs during isotopic analysis as well as any isotopic fractionation that may occur during purification of the sample (see below). After spiking, each sample was acidified to attain a pH of about 2, then passed through a column of AG1-X8 anion exchange resin, onto which the Cr(VI) was adsorbed. Any dissolved Cr(III), other cations, and weak acid anions were eluted with dilute HCl. Cr(VI) was then converted to Cr(III) with a sulfurous acid solution and eluted. Sulfate and most other anions were removed by passing the solution through a second anion exchange column. Blank samples were routinely processed in parallel with the study samples. The amount of Cr found in these blanks was less than 8 ng in all cases,

and was usually less than 5 ng. Very little Cr(III) was present in most of the filtered sample solutions because of the limited solubility of $\text{Cr}(\text{OH})_{3(s)}$ in the experiments. Accordingly, the potential for contamination of the desired Cr(VI) fraction by the Cr(III) from the experiment was negligible in most cases (see discussion for exceptions).

Mass-dependent isotopic fractionation occurs during mass spectrometry and induces a systematic mass bias that must be corrected for. We used the double spike method to correct for mass bias and any isotopic fractionation induced by sample preparation. This approach has been described in detail elsewhere ([Compston and Oversby, 1969](#); [Johnson and Beard, 1999](#)). Briefly, the spike solution's $^{54}\text{Cr}/^{50}\text{Cr}$ ratio is well calibrated. The measured $^{54}\text{Cr}/^{50}\text{Cr}$ ratio of the sample-spike mixture is highly sensitive to the mass bias, which can be extracted from the measured data using iterative calculations that mathematically separate the spike and sample contributions.

Mass spectrometry was carried out using either a thermal ionization mass spectrometry (TIMS) method ([Ellis et al., 2002](#)) or a multicollector ICP–MS method ([Schoenberg et al., 2008](#)). TIMS was used for samples from the preliminary Fe(II) experiments and the mandelic acid experiments. The analyses were done using a Finnigan MAT 261 multicollector thermal ionization mass spectrometer at the US Geological Survey in Menlo Park, CA, USA. Five hundred nanograms Cr was loaded as CrCl_3 , with boric acid and silica gel, onto a Re filament. The ratios $^{50}\text{Cr}/^{52}\text{Cr}$, $^{53}\text{Cr}/^{52}\text{Cr}$, and $^{54}\text{Cr}/^{52}\text{Cr}$ were measured simultaneously a minimum of 50 times, in blocks of 10 measurements, between which detector baselines were measured. Outliers were removed and the results of each block were fed into a spreadsheet-based routine that performed the double spike data reduction and extracted final results from the measured ratios. Based on results from samples prepared and analyzed in duplicate, precision for the TIMS analyses was 0.20% (2σ).

A multicollector ICP–MS method very similar that of [Schoenberg et al. \(2008\)](#) was used to analyze samples from the final Fe(II) experiments and the humic substance experiments. Measurements were made using a Nu Plasma HR instrument. Samples were dissolved in 0.28 M HNO_3 to attain roughly 300 ng/mL Cr and were introduced into the instrument via a desolvating nebulizer (DSN-100; Nu Instruments). ArC^+ and ArN^+ interferences were avoided using a high resolution method described by [Weyer and Schwieters \(2003\)](#). ^{56}Fe , ^{51}V , and ^{49}Ti intensities were measured, and corrections for ^{54}Fe , ^{50}V , and ^{50}Ti were calculated and applied, taking into account the mass bias determined from the Cr double spike. Because the value obtained on the SRM-979 standard varies slightly from day to day, presumably because of variability in the mass bias law of the instrument ([Albarède and Beard, 2004](#)), sample results were normalized to the average value for each day ([Schoenberg et al., 2008](#)). Duplicate preparation and analysis of samples indicate the uncertainty for these analyses was $\pm 0.16\%$ (2σ).

2.5. Extraction of isotopic fractionation factors from data

If Cr(VI) reduction proceeds in a well mixed, closed system with a constant isotopic fractionation factor, the $\delta^{53}\text{C}$

value of the remaining Cr(VI) can be modeled using a Rayleigh distillation equation, which can be expressed

$$\delta(t) = (\delta_0 + 1000\text{‰}) \left(\frac{c(t)}{c_0} \right)^{\alpha-1} - 1000\text{‰} \quad (5)$$

where $c(t)$ and $\delta(t)$ are the concentration and isotopic composition of Cr(VI) as functions of time and c_0 and δ_0 are initial values. Eq. (5) can be rearranged to give the linear form:

$$\ln(\delta(t) + 1000\text{‰}) = (\alpha - 1) \ln[c(t)] + [\ln(\delta_0 + 1000\text{‰}) - (\alpha - 1) \ln(c_0)] \quad (6)$$

Best fit α values were found by creating plots of $\ln(\delta^{53}\text{Cr} + 1000\text{‰})$ vs. $\ln[c(t)]$, determining the best fit line's slope via linear regression, and calculating α from the slope. This is equivalent to the approach advocated by Scott et al. (2004). Uncertainties in ε were calculated by propagating the standard errors of the best-fit slopes through the calculations and doubling the result.

3. RESULTS

3.1. Cr(VI) reduction by dissolved Fe(II): rate experiments

Results of the two experiments exploring rates of Cr(VI) reduction by Fe(II) at pH = 5.0 and 5.3 are displayed in Fig. 1 (no isotopic data were generated from these experiments). After the first few minutes of reaction, reaction rates are slightly slower than those predicted using the rate law of Buerge and Hug (1997). However, reduction proceeded much faster than predicted by this rate law during the first 3 min; steep decreases are visible in Fig. 1. Attempts to perform a similar experiment at pH = 6 revealed nearly complete reduction in the first few minutes (data not shown). Apparently, reaction kinetics were accelerated during the mixing of the reagents and/or immediately thereafter. These rate experiments were carried out using the lower Fe(II) concentrations and faster mixing methods of the final experiments, and are not representative of the preliminary

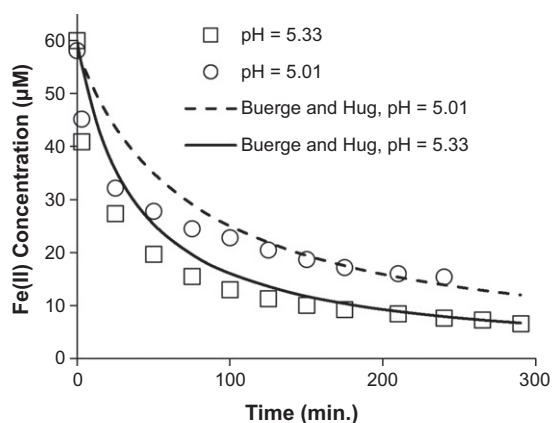


Fig. 1. Rates of reaction after injection of Fe(II) into Cr(VI)-bearing solutions buffered at pH = 5.0 (circles) and 5.3 (squares), and rate predictions based on the model of Buerge and Hug (1997) for pH = 5.0 (dashed line) and 5.3 (solid line). Reduction during the first few minutes was faster than model predictions.

experiments. Those were carried out with greater injected Fe(II) concentrations and slower mixing.

3.2. Cr(VI) reduction by dissolved Fe(II): preliminary isotopic experiments

$\delta^{53}\text{Cr}$ results from the preliminary Fe(II)-driven reduction experiments are given in Table 1 and Fig. 2. The progression of Cr(VI) concentration during the 24 h reaction time after each Fe(II) addition was not monitored, as each step was designed to proceed to completion and only the final Cr(VI) concentration was determined. In each experiment, Cr(VI) was reduced by three successive additions of Fe(II), which reduced about 20%, 40%, and 20% of the Cr(VI), respectively, and together resulted in reduction of about 80%.

$\delta^{53}\text{Cr}$ of the remaining dissolved Cr(VI) increased as its concentration decreased; Cr(VI) became enriched in the heavier isotope as reduction proceeded (Fig. 2). The data fall close to Rayleigh distillation models (Eq. (5)), though the pH = 6 data deviate from the model slightly more than the analytical uncertainty. The best-fit models for the experiments at pH = 4.0, 5.0, and 6.0 yielded isotopic fractionation, expressed as ε values, of -4.19‰ , -3.65‰ , and -2.97‰ , respectively.

3.3. Cr(VI) reduction by dissolved Fe(II): final isotopic experiments

Results from the final Fe(II)-driven reduction experiments are given in Table 2. These experiments were conducted with lower injected Fe(II) concentration and faster mixing, and the Fe(II) solution was added in 5 steps. Each decrease in Cr(VI) concentration, determined after the complete consumption of the added Fe(II), was found to be equal to that predicted by the reaction stoichiometry; the molar ratio of Cr(VI) loss to Fe(II) added was 1:3 within the uncertainties of the measurements. This indicated that the reaction had consumed all added Fe(II). Control experiments without added Fe(II) showed no significant decrease in Cr(VI).

In Fig. 3, $\delta^{53}\text{Cr}$ is plotted vs. the extent of Cr(VI) reduction in the final Fe(II)-driven reduction experiments. The data from the three experiments at three different pH values fall close to a single Rayleigh distillation model, with no significant differences among the isotopic fractionation factors determined for the individual experiments. The ε values and their uncertainties, derived from best-fit Rayleigh models, are given in Table 3. These results are identical to the result from the preliminary pH = 4.0 experiment, within the uncertainties. A single Rayleigh model fit to the data from all three final experiments and the preliminary pH = 4 experiment attains a close fit to all the data and yields an ε value of -4.20‰ (Fig. 3).

3.4. Cr(VI) reduction by dissolved humic substances

Time courses of Cr(VI) concentrations during reduction by the three humic substances are given in Fig. 4. Reaction rates were very slow compared to the Cr(VI)–Fe(II)

Table 1
Results of preliminary experiments, with Fe(II) injected at higher concentration.

	pH = 4.0		pH = 5.0		pH = 6.0	
	Cr(VI) (μM)	$\delta^{53}\text{Cr}$ (‰)	Cr(VI) (μM)	$\delta^{53}\text{Cr}$ (‰)	Cr(VI) (μM)	$\delta^{53}\text{Cr}$ (‰)
Initial	21.7	-0.53	21.7	-0.50, -0.45*	22.2	-0.57
Step 1	18.7	N.D.	18.0	0.46	19.5	0.14
Step 2	10.4	2.77, 2.85*	10.3	2.26	9.6	1.75
Step 3	4.3	6.30	4.5	5.36	4.7	4.23

N.D.: not determined.

* Duplicate preparation and measurement.

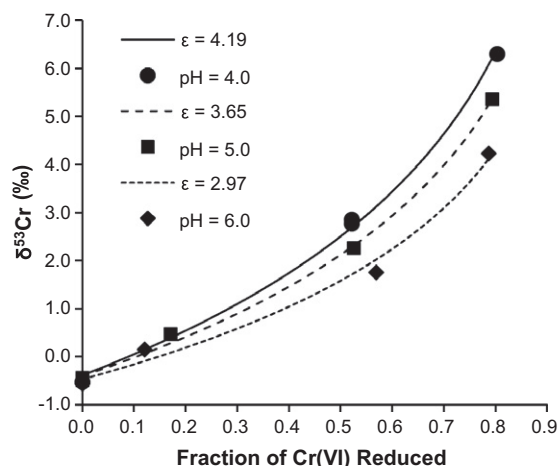


Fig. 2. Enrichment of Cr(VI) in the heavier isotope as a function of the extent of reduction in preliminary Fe(II)-driven reduction experiments at pH = 4.0 (circles), 5.0 (squares), and 6.0 (diamonds). Uncertainties are close to the sizes of the symbols.

reaction, and were broadly consistent with those reported by Wittbrodt and Palmer (1996). Concentrations conformed roughly to pseudo-first order kinetics, with Cr(VI) half-lives of 177–390 h, after the first 24 h of reduction. During the first 24 h, rates are somewhat greater than those of the pseudo-first order models fitting later time points.

In Fig. 5, $\delta^{53}\text{Cr}$ is plotted vs. the extent of Cr(VI) reduction. Most data (15 out of 18 points) fall close to a single Rayleigh distillation model with $\epsilon = -3.11\text{‰}$. However, each experiment's final data point, with >93% reduction of the initial Cr(VI), falls significantly below the trend defined by the other data. A sample preparation problem is likely (see Section 4), so we excluded these data when determining best-fit Rayleigh models. The resulting ϵ values for

Table 2
Results of the final Fe(II)-driven reduction experiments.

	pH = 4.5		pH = 5.0		pH = 5.3	
	Cr(VI) (μM)	$\delta^{53}\text{Cr}$ (‰)	Cr(VI) (μM)	$\delta^{53}\text{Cr}$ (‰)	Cr(VI) (μM)	$\delta^{53}\text{Cr}$ (‰)
Initial	20.5	0.16	20.5	0.16	20.5	0.16
Step 1	13.6	1.73	13.6	1.80	13.5	1.79
Step 2	8.4	4.19	8.4	3.82	8.4	3.88
Step 3	5.1	6.30	5.0	6.11	5.2	6.34
Step 4	3.2	8.01	3.3	8.02	3.1	7.55
Step 5	1.9	10.47	1.8	10.06	1.9	10.22

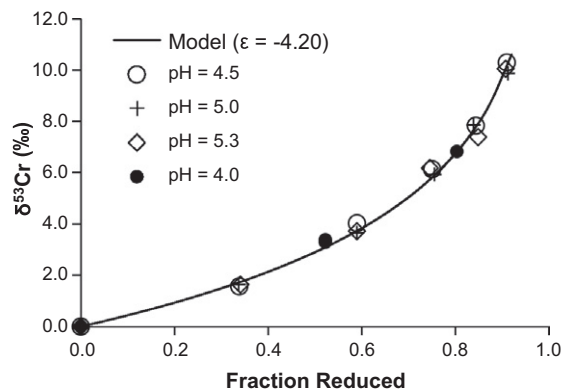


Fig. 3. Isotope data for the three final Fe(II)-driven reduction experiments (open symbols, given in legend) and the preliminary experiment at pH = 4.0 (filled circles). Data from all four experiments conform to a single Rayleigh distillation model with $\epsilon = -4.20\text{‰}$ (solid line). Uncertainties are close to the sizes of the symbols.

the three experiments individually, and their uncertainties, are given in Table 3. No significant differences exist between the three ϵ values.

3.5. Cr(VI) reduction by mandelic acid with oxide catalysts

Cr(VI) concentrations during goethite- and Al_2O_3 -catalyzed reduction by mandelic acid at pH = 4.0 are plotted in Fig. 4. As expected, loss of some of the initial dissolved Cr(VI) from solution occurred via adsorption during the 24-h equilibration time prior to addition of the reductant. Decrease in Cr(VI) concentration was about 35% with both catalysts (Fig. 4); this is consistent with the observations of Deng and Stone (1996). After addition of the reductant,

Table 3

Isotopic fractionation factors derived from experiments that were unaffected by the diffusive barrier effect.

Reductant	Initial reductant concentration	pH	Catalyst	ϵ^a (‰)
Dissolved Fe(II)	9–25 μ M	4.0	–	-4.19 ± 0.31
Dissolved Fe(II)	5–20 μ M	4.5	–	-4.28 ± 0.18
Dissolved Fe(II)	5–20 μ M	5.0	–	-4.15 ± 0.18
Dissolved Fe(II)	5–20 μ M	5.3	–	-4.16 ± 0.35
Dissolved Fe(II)	All above, combined			-4.20 ± 0.11
Elliot fulvic acid	100 mg/L	5.0	–	-3.14 ± 0.27
Waskish humic acid	100 mg/L	4.5	–	-3.09 ± 0.20
Waskish humic acid	100 mg/L	5.0	–	-3.08 ± 0.07
Mandelic acid	200 μ M	4.0	Goethite	-3.10 ± 0.23
Mandelic acid	200 μ M	4.0	γ -Al ₂ O ₃	-2.98 ± 0.46
All organic reductant experiments, combined				-3.11 ± 0.11

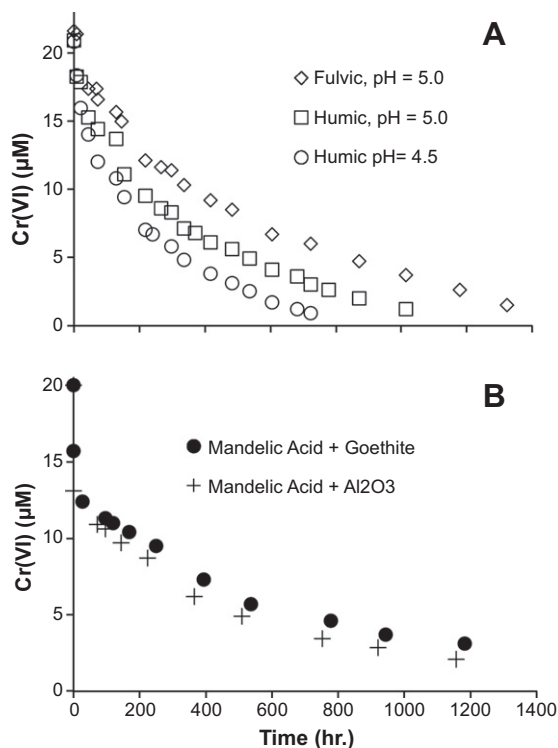
^a Uncertainties were calculated from 2 times the standard error of the slope- see Eq. (6).

Fig. 4. Reduction of Cr(VI) by organic reductants. (A) 100 mg/L humic substances: Elliott Soil Fulvic Acid (open diamonds) at pH = 5.0, Waskish Peat Humic Acid at pH = 5.0 (open squares), and Waskish Peat Humic Acid at pH = 4.5 (open circles); (B) 0.2 mM Mandelic acid at pH = 4.0, with 0.2 g/L goethite (closed circles) or 1.0 g/L alumina (crosses) as catalysts. In B, the two points plotted at zero time for each experiment give the concentration before and after equilibration with the solid.

dissolved Cr(VI) concentration decreased smoothly, roughly following pseudo-first order models with half-lives of 550 and 435 h for the goethite- and alumina-bearing experiments, respectively. Control experiments without catalyst showed no significant Cr(VI) reduction by mandelic acid at pH 4 (data not shown).

The $\delta^{53}\text{Cr}$ data from the mandelic acid experiments show results very close to those of the humic substances

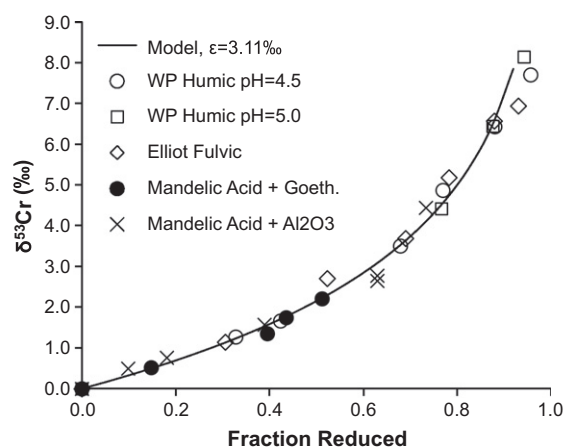


Fig. 5. Cr isotope results from experiments with organic reductants. The three points with fraction reduced greater than 0.93 were excluded in deriving the best-fit Rayleigh model (solid line).

experiments (Fig. 5). Table 3 gives the ϵ value derived from each mandelic acid experiment, and also that of the best-fit model for all of the organic reductant experiments combined (once again excluding the last set of humic substance data points). Fig. 5 shows that the data fall close to a single model with $\epsilon = -3.11\text{‰}$. Some data points deviate from the model beyond the analytical uncertainty, suggesting there may be slight differences in ϵ between the various experiments. However, the deviations are small (none greater than 0.4‰) so any corresponding differences in ϵ are small. Furthermore, differences in ϵ between experiments do not exceed the uncertainties derived from the data regressions (Table 3).

4. DISCUSSION

4.1. Heterogeneity and diffusive barrier effects in the dissolved Fe(II) experiments

In a Cr(VI) reduction experiment with a very high reaction rate, significant reaction may occur before the injected Fe(II) is evenly mixed into the solution. In this section, we

argue that this heterogeneous reaction regime, when it occurs, causes the ϵ value observed at the system scale to be an “effective” ϵ that is smaller in magnitude than the “intrinsic” ϵ of the reaction at any given point. This phenomenon can be understood by considering the diffusive interface at the outer edge of a droplet of Fe(II) solution injected into the Cr(VI) solution. Reaction occurs as Cr(VI) diffuses into the Fe(II) solution and vice versa.

Fig. 6 depicts an idealized, quantitative, one dimensional model, in which Cr(VI) diffuses into an Fe(II)-bearing zone and is reduced. This model makes two simplifying approximations: (1) It considers a steady state case with constant Cr(VI) concentration and $\delta^{53}\text{Cr}$ at the outer boundary of the Fe(II)-rich zone; (2) Cr(VI) reduction follows first-order kinetics (i.e., Fe(II) concentration is held spatially invariant). This model was developed, and applied in a different context, by Bender (1990) and Clark and Johnson (2008), who presented an analytical solution to the diffusion–reaction governing equations. This solution is plotted in Fig. 6.

With increasing distance into the Fe(II)-bearing zone, the concentration of Cr(VI) decreases and its $\delta^{53}\text{Cr}$ value increases, because the Cr(VI) is being consumed and isotopically fractionated by reduction and is increasingly separated from the supply of Cr(VI) outside the zone. The $\delta^{53}\text{Cr}$ value of the Cr(III) produced follows that of Cr(VI), offset by ϵ , and becomes substantially elevated deep inside the Fe(II)-bearing zone (Fig. 6). This is the key point: The average Cr(III) produced is isotopically heavier (i.e., not as strongly fractionated) compared to the case where the Cr(VI) and Fe(II) are fully mixed and a diffusive barrier does not exist between them. In the example shown in

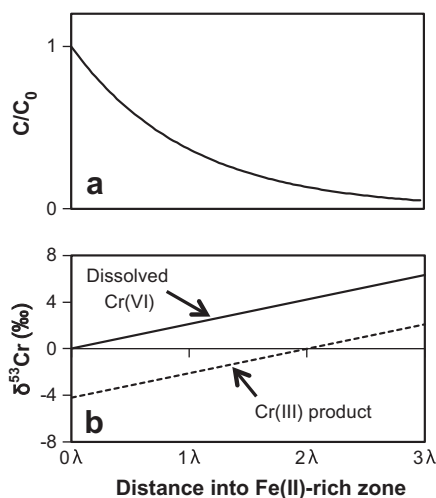


Fig. 6. Idealized, steady-state model of Cr(VI) reduction at the diffusive interface between an Fe(II)-bearing solution and a Cr(VI)-bearing solution. The model assumes first-order Cr(VI) reduction (i.e., constant Fe(II) concentration). The outer edge of the Fe(II) bearing zone is at distance = 0, where Cr(VI) concentration is fixed at C_0 and $\delta^{53}\text{Cr}$ is fixed at 0‰. (a) Dissolved Cr(VI) concentration versus distance into the Fe(II)-bearing zone, expressed in units of $\lambda = \sqrt{D/k}$, where D is the diffusivity of Cr(VI) and k is the first order reaction rate constant. $\lambda \approx 0.1$ mm if $k = 0.1$ s $^{-1}$. (b) $\delta^{53}\text{Cr}$ of dissolved Cr(VI) (solid line) and the reaction product (dashed line) for $\epsilon = -4.2$ ‰.

Fig. 6, the spatially integrated, mass-weighted $\delta^{53}\text{Cr}$ for the Cr(III) produced is -2.1 ‰, whereas the $\delta^{53}\text{Cr}$ of the Cr(VI) supplied from the bulk solution outside the Fe(II)-bearing zone is 0.0‰. Accordingly, the “effective” isotopic fractionation observed at the system scale is -2.1 ‰, despite the fact that ϵ for the reaction itself (the “intrinsic” fractionation) was set at -4.2 ‰. We call this weakening of the observed isotopic fractionation relative to the intrinsic fractionation a “diffusive barrier effect”. The effect has been observed previously in the context of isotopic fractionation of NO_3^- , O_2 , and SeO_4^{2-} in ocean or wetland waters diffusively connected to reduction reactions in underlying sediments (Bender, 1990; Brandes and Devol, 1997; Clark and Johnson, 2008).

A more accurate model of the interactions when an Fe(II) solution is injected into a Cr(VI) solution would account for spatially varying Fe(II) concentration and would address the transient nature of the Cr(VI)–Fe(II) reaction zone, which becomes more diffuse over time. However, even with these modifications, the key aspects of the model would remain qualitatively the same as those depicted in Fig. 6: Cr(VI) inside the Fe-rich zone would still be isotopically heavier than the bulk solution outside, because reduction drives the Cr(VI) to greater $\delta^{53}\text{Cr}$ values and a diffusive barrier limits equilibration with the exterior. A diffusive barrier effect is inescapable if significant reaction occurs while the injected Fe(II) solution is present as separate domains not yet fully mixed with the bulk solution.

Under the conditions present immediately after Fe(II) injection into our preliminary pH = 5.0 and 6.0 experiments, diffusive barrier effects could have occurred. According to Buerge and Hug (1997), the rate of Cr(VI) reduction by aqueous Fe(II) is proportional to Fe(II) concentration and strongly pH-dependent, with the rate ten times greater at pH 6.0 compared to pH = 5.0, and six times greater at pH = 5.0 compared to pH = 4.0. The preliminary experiments had much greater injected Fe(II) concentrations than the final experiments and thus had much faster reaction rates at the edges of the injected Fe(II) solution. Additionally, less attention was paid to immediate mixing after injection. Using the Buerge and Hug (1997) rate model, we calculate fast reduction rates (significant reaction within several seconds) for the injected 10 mM Fe(II) solution at pH = 5.0 and 6.0. In comparison, mixing was begun by hand after injection, and may have taken more than about one minute. We thus conclude that diffusive barrier effects were likely in these experiments, and should have been stronger at pH = 6.0 than at pH = 5.0. At pH 4.0, however, the reaction was several times slower than at pH = 5.0, and therefore we expect mixing was complete prior to significant reaction.

The final experiments were designed to avoid diffusive barrier effects. Mixing was much faster and Fe(II) concentrations in the injected solutions were one tenth those of the preliminary experiments. The lower Fe(II) concentrations greatly decreased reaction rates during the time period when the Fe(II) was incompletely mixed into the experimental solution. Fig. 1 shows the reaction rates experiments that demonstrated this; at pH = 5.3 and 5.0, 32% and 22%, respectively, of the Cr(VI) was lost in the first three minutes. Given that mixing was complete within about

ten seconds in the final experiments, this reaction rate should have been sufficiently slow to avoid diffusive barrier effects.

A comparison between our preliminary and final experiments at pH = 5.0 provides strong evidence for a diffusive barrier effect in the preliminary one. These two experiments were nearly identical: The masses of Fe(II) delivered were similar, and other solution variables were identical. The greater mixing rate and more dilute Fe(II) stock solution used in the final experiment created ephemeral differences, relative to the preliminary experiment, that existed only in the brief time period prior to complete mixing. The different isotopic results indicate a difference in reaction dynamics during that time period, and there are very few ways to explain such a difference. The diffusive barrier effect we describe above is a viable explanation, and the conditions in the preliminary experiment were such that it likely occurred. We considered the alternative hypothesis that the injected Fe(II) concentration itself was the controlling variable, but this fails to explain the apparent lack of diffusive barrier effects in the preliminary pH = 4.0 experiment.

Table 3 lists the fractionation factors derived from the four experiments that we believe were not affected by diffusive barrier effects: These are the three final experiments (pH = 4.5, 5.0, and 5.3) and the preliminary pH = 4.0 experiment. All data points from these experiments conform to a single ϵ value of -4.20‰ ($\pm 0.11\text{‰}$). This consistent result provides additional confidence that we have observed the intrinsic fractionation factor without significant diffusive barrier effects. If such effects were involved, we would expect variability in our results depending on differences in reaction and mixing rates.

4.2. Integration with a previous study of Fe(II)-driven Cr(VI) reduction

Døssing et al. (2011) recently reported Cr isotope isotopic fractionation factors for homogenous Cr(VI) reduction by dissolved Fe(II). Three nominally identical batch experiments (designated R1), carried out with 1.1 mM Fe(II) injected into a 38 mM Cr(VI) solution initially at pH = 7.0, yielded conflicting results. Rayleigh model interpretations of their data give $\epsilon = -4.4 \pm 0.3\text{‰}$, $-3.0 \pm 0.1\text{‰}$, and $-3.0 \pm 0.3\text{‰}$ for the three experiments. Because the initial pH was 7.0, the reaction rate must have been very fast (Buerge and Hug, 1997) and thus Cr(VI) reduction might have occurred before homogenization of the experiments, leading to diffusive barrier effects. The differences between the results of their three experiments may have been caused by inadvertent differences in the way the injected Fe(II) solution was mixed into the experiment. We suggest that the result from the first R1 experiment, which yielded the strongest fractionation, is closest to the intrinsic fractionation, whereas the other R1 experiments yielded lesser effective values because of diffusive barrier effects.

Their first experiment's result of -4.4‰ is statistically indistinguishable from our results. Speculatively, we hypothesize that this result was not affected significantly by diffusive limitation, and the intrinsic ϵ for homogeneous Cr(VI) reduction by aqueous Fe(II) is close to 4.2‰ across the pH

range 4.0–7.0. However, additional experiments, designed specifically to assure that diffusive barrier effects do not occur, would be needed above pH = 5.3 to test that hypothesis.

Although the intrinsic isotopic fractionation is of fundamental importance, in real geochemical settings, the effective fractionation governs the isotopic compositions observed on the system scale. Effective fractionation in nature will vary just as it did in our experiments and those of Døssing et al. (2011), according to the reaction-transport dynamics of each system. Furthermore, as demonstrated by the R2 and R3 experiments of Døssing et al. (2011), isotopic fractionation can be greatly influenced by the presence of solid phases like green rust (e.g., $\epsilon = -1.5\text{‰}$). Accordingly, a detailed understanding of reaction mechanisms, solid phase reductants, and reactive transport parameters is required in order to precisely estimate fractionation factors for real systems. If such understanding is lacking, one must incorporate considerable uncertainty into the effective fractionation factors used to interpret data.

4.3. Adsorption, solid phases, and species separation issues in our experiments

The fact that a substantial fraction of the Cr(VI) was adsorbed onto solids in the oxide-catalyzed mandelic acid-driven reduction experiments should have no effect on our data interpretation, provided three conditions are met: First, we assume there is no significant isotopic fractionation accompanying adsorption or desorption, as has been demonstrated by Ellis et al. (2004). Second, we assume the adsorbed and dissolved Cr(VI) exchanged with each other and remained isotopically identical as the system slowly evolved over >100 h. Finally, we assume the ratio of adsorbed Cr(VI) to dissolved Cr(VI) remained constant during the experiment. We believe all of these assumptions are correct, and the dissolved Cr(VI) we measured was representative of the total Cr(VI) pool, in terms of both isotopic composition and extent of reduction.

We considered the yellowish precipitate that formed in our Fe(II)-driven reduction experiments as a possible complicating factor. First, this precipitate could remove Cr(VI) from solution via adsorption/coprecipitation without reduction. However, the amount of Cr(VI) adsorbed was very small, because the mass of precipitate was very small. The total amount of Fe(III) generated in each experiment was less than 60 μM ; in the early phases, much less was present. In comparison, our mandelic acid experiment had 38 times more Fe(III) present (2250 $\mu\text{mol/L}$), as a very fine Goethite suspension. In that experiment, 35% of the Cr(VI) adsorbed to the surfaces. Thus, in our Fe(II)-driven experiments, the fraction of Cr(VI) adsorbed onto the ferric precipitate must have been small. More importantly, the loss of Cr(VI) from solution in our final set of experiments precisely matched the calculated amount reduced, based on the reaction stoichiometry and the measured Fe(II) additions. Thus Cr(VI) removal was driven by reduction, with insignificant removal via coprecipitation.

The presence of the ferric precipitate in the experiments may have allowed Cr(VI) reduction to occur partially as a surface-catalyzed reaction rather than as an aqueous phase

reaction alone. [Buerge and Hug \(1999\)](#) reported that the presence of 1100 $\mu\text{mol/L}$ lepidocrocite induced a threefold increase in the rate of Cr(VI) reduction by Fe(II). In our experiments, the amount of Fe(III) present was about 20 times less than that at the end of the experiments, and about 100 times less toward the beginning. Accordingly, we infer that the Fe(III) solid had little effect on the reaction rate and mechanisms in our experiments, especially in the early stages of each one. More importantly, if surface-mediated reaction mechanisms had a significant effect on ϵ , this effect would have been small in the early stages of each experiment, and would have increased with successive additions of Fe(II), as the Fe(III) reaction product increased in mass. Our data show no evidence for changes in ϵ ([Fig. 3](#)), and we conclude that the small amount of precipitate that formed over time did not significantly affect ϵ .

We excluded, from regressions to determine ϵ , the final data point of each humic substance experiment because we suspected a small fraction of the Cr(III) in each sample contaminated the Cr(VI) fraction that was purified for analysis. Because the extent of reduction was greater than 93%, the Cr(III) mass in each sample was at least 13 times greater than the Cr(VI) mass. We assume some or all of this Cr(III) was complexed with various functional groups of the humic or fulvic acids. Because the humic and fulvic acids are diverse mixtures, small fractions of them likely have properties that allow them to follow the Cr(VI) through the ion exchange procedure. We calculate that, at most, a cross-contamination of 1.5% of the Cr(III) into the analyzed Cr(VI) fraction is needed to explain the offsets observed. Such a contamination is possible, if not expected, during the ion exchange procedures when humic substances are present to complex Cr(III), and thus we believe the exclusion of the three data points is warranted. It is also possible that the three data points at 88% reduction are affected by this problem, though to a much smaller extent. If those points are also excluded, the remaining data from the three humic/fulvic acid experiments together yield an ϵ value of $-3.23 \pm 0.17\text{‰}$ (versus $-3.10 \pm 0.13\text{‰}$ with the points included). Because the 88% reduction data are not clearly shifted, we chose to report the regression result obtained when they are included.

4.4. Relationship between Cr isotopic fractionation and reduction mechanisms

Kinetic fractionation factors are known to depend on the exact nature of the reaction, including the characteristics of intermediate species within the overall reaction, and the relative rates of the elementary reaction steps ([Rees, 1973](#); [Schauble et al., 2004](#)). In the present case, Cr(VI) reduction proceeds in multiple electron transfer steps, with Cr(V) and/or Cr(IV) species as ephemeral intermediates, and transfers of either one or two electrons at each step, depending on the nature of the reductant ([Westheimer, 1949](#); [Espenson, 1970](#); [Elovitz and Fish, 1995](#); [Wittbrodt and Palmer, 1996](#); [Zink et al., 2010](#)).

The clear difference in isotopic fractionation factor between Cr(VI) reduction driven by dissolved Fe(II) and that driven by organic reductants invites speculation regarding a

systematic relationship between reaction mechanism and ϵ . Because each Fe(II) donates only one electron, Fe(II)-driven reduction involves at least three steps and both Cr(V) and/or Cr(IV) intermediate species. Organic reductants, however, can donate one or two electrons at a time ([Westheimer, 1949](#)) and thus the reaction mechanism can be quite different, perhaps bypassing either the Cr(IV) or Cr(V) intermediate. The fact that the three organic reductants in the study induce essentially the same amount of isotopic fractionation, despite differences between the reductants, suggests some commonality of reaction mechanism. For example, the organic reductants may tend to transfer two electrons to begin Cr(VI) reduction, whereas each Fe(II) can only transfer one. The very different reaction rates, with Fe(II)–Cr(VI) reactions proceeding hundreds of times faster than the organic–Cr(VI) reactions, also suggest contrasting mechanisms that may be related to the contrasting isotopic fractionations. The initial Fe(II)–Cr(VI) electron transfer is very quick, in part because it involves no change of coordination: The Fe and Cr remain in octahedral and tetrahedral coordination, respectively ([Espenson, 1970](#)). In contrast, the initial organic–Cr(VI) electron transfer involves rearrangement of multiple covalent bonds in the organic molecule ([Westheimer, 1949](#)), leading to much slower reaction kinetics. Although the kinetic details and their effects on isotopic fractionation are not worked out yet, there appear to be systematic reaction mechanism differences that are consistent with our experimental results. Alternatively, mass transfer limitations (e.g., barriers to binding of Cr(VI) to the organic molecules) could lead to the difference in isotopic fractionation. We speculatively suggest that organic reductants as a class may induce less Cr isotope fractionation than aqueous Fe(II) does, but more data would be needed to develop a secure systematic understanding.

Interestingly, in Cr(VI) reduction by magnetite, where the reductant is crystal-bound Fe(II), $\epsilon = -3.5\text{‰}$ ([Ellis et al., 2002](#)), 20% less than our result of -4.2‰ for aqueous Fe(II). Apparently, the surface-related reaction mechanism of the magnetite reaction involves different intermediate species and/or rates for reaction steps compared to the aqueous Fe(II) mechanism. Also interesting is the comparison between microbial Cr(VI) reduction under electron donor-poor conditions ($\epsilon = -4.1\text{‰}$; [Sikora et al., 2008](#)), and our result for aqueous Fe(II)-driven reduction ($\epsilon = -4.2\text{‰}$). This similarity could conceivably arise from some systematic phenomenon, but we do not have enough evidence to support such ideas. Overall, systematic relationships between Cr isotope fractionation and Cr(VI) reduction mechanisms would be quite useful, but at present, we see no reliable systematic patterns.

5. CONCLUSIONS

Our experiments with homogeneous Cr(VI) reduction by dissolved Fe(II) indicate Cr isotopic fractionation, expressed as ϵ , of $-4.20 \pm 0.11\text{‰}$, over the pH range 4.0–5.3 at room temperature. This agrees, within the uncertainties, with the result from one experiment by [Døssing et al. \(2011\)](#) at pH = 7.0.

Some of our preliminary, less refined experiments yielded lesser ϵ values. We believe these lower values were a result of diffusive barrier effects, in which rapid, diffusion-limited reaction occurred prior to complete mixing of reactants. We suggest that, in any experiment where reaction progresses significantly prior to complete mixing of reactants, the isotopic fractionation observed at the system scale may be an effective fractionation that is weaker than the intrinsic fractionation induced by the reaction kinetics.

This issue is relevant in natural systems also. Whenever a Cr(VI)-bearing solution comes into contact with Fe(II)-rich waters, for example in a redox-stratified ocean of the proterozoic, reduction is likely to proceed more rapidly than physical mixing. As a result, diffusion limitations will tend to occur, leading to effective fractionation, manifested at the system scale, that is smaller in magnitude than the intrinsic fractionation.

Our experiments with three organic reductants, including oxide surface-catalyzed experiments, all conform to a single fractionation factor, with $\epsilon = -3.11 \pm 0.11\%$. The experiments covered a limited range of pH (4.0–5.0). Further experiments are needed to cover a broader range of conditions, but the lack of pH-dependency observed so far suggests this result may apply over a wider range of pH.

These results, combined with previously published determinations of isotopic fractionation for a variety of Cr(VI) reduction mechanisms, can improve interpretation of $\delta^{53}\text{Cr}$ data. For example, in a groundwater system where Cr(VI) reduction is known to occur via homogeneous reaction with dilute Fe(II), an estimate of $\epsilon = -4.2$ for the intrinsic isotopic fractionation would be appropriate. Alternatively, if nothing is known about reduction mechanisms in the system, a range of possible values reflecting those observed in published laboratory studies with various reductants (e.g., $\epsilon = -1.5\%$ to -4.5%) should be considered.

Similarly, in paleo-redox studies using $\delta^{53}\text{Cr}$, improved understanding of isotopic fractionation during Cr(VI) reduction by Fe(II) is helpful. For example, if reduction of Cr(VI) in contact with Fe-rich archaean ocean waters was driven by homogeneous, aqueous phase interaction, the intrinsic fractionation might be estimated at $\epsilon = -4.2$. However, in Fe(II)-rich waters, alternative reaction pathways such as reaction with green rust likely lead to smaller magnitudes of intrinsic fractionation, and system-scale reactive transport dynamics will also affect the isotopic differences observed (Døssing et al., 2011).

ACKNOWLEDGEMENTS

This material is based upon work supported by the National Science Foundation under Grants EAR 02-29079, EAR 07-32481, and EAR 03-20597.

REFERENCES

Albarède F. and Beard B. L. (2004) Analytical methods for non-traditional isotopes. In *Geochemistry of Non-Traditional Stable Isotopes* (eds. C. M. Johnson, B. L. Beard and F. Albarède). Mineralogical Society of America, Washington, pp. 113–152.

- Ball J. W. and Nordstrom D. K. (1998) Critical evaluation and selection of standard state thermodynamic properties for chromium metal and its aqueous ions, hydrolysis species, oxides, and hydroxides. *J. Chem. Eng. Data* **43**, 895–918.
- Basu A. and Johnson T. M. (2012) Determination of hexavalent chromium reduction using Cr stable isotopes: Isotopic fractionation factors for permeable reactive barrier materials. *Environ. Sci. Technol.* <http://dx.doi.org/10.1021/es204086y>.
- Bender M. L. (1990) The $\delta^{18}\text{O}$ of dissolved O_2 in seawater: a unique tracer of circulation and respiration in the deep sea. *J. Geophys. Res.* **95**, 22243–22252.
- Berna E. C., Johnson T. M., Makdisi R. S. and Basu A. (2010) Cr stable isotopes as indicators of Cr(VI) reduction in groundwater: a detailed time-series study of a point-source plume. *Environ. Sci. Technol.* **44**, 1043–1048.
- Blowes D. W., Ptacek C. J., Benner S. G., McRae C. W. T., Bennett T. A. and Bennett R. W. (2000) Treatment of inorganic contaminants using permeable reactive barriers. *J. Contam. Hydrol.* **45**, 123–137.
- Brandes J. A. and Devol A. H. (1997) Isotopic fractionation of oxygen and nitrogen in coastal marine sediments. *Geochim. Cosmochim. Acta* **61**, 1793–1801.
- Buerge I. J. and Hug S. J. (1997) Kinetics and pH dependence of Cr(VI) reduction by Iron(II). *Environ. Sci. Technol.* **31**, 1426–1432.
- Buerge I. J. and Hug S. J. (1999) Influence of mineral surfaces on Cr(VI) reduction by Iron(II). *Environ. Sci. Technol.* **33**, 4285–4291.
- Clark S. K. and Johnson T. M. (2008) Effective isotopic fractionation factors for solute removal by reactive sediments: a laboratory microcosm and slurry study. *Environ. Sci. Technol.* **42**, 7850–7855.
- Compston W. and Oversby V. M. (1969) Lead isotopic analysis using a double spike. *J. Geophys. Res.* **74**, 4338–4348.
- Deng B. and Stone A. (1996) Surface-catalyzed Cr(VI) reduction: reactivity comparisons of different organic reductants and different oxide surfaces. *Environ. Sci. Technol.* **30**, 2484–2494.
- Døssing L. N., Dideriksen K., Stipp S. L. S. and Frei R. (2011) Reduction of hexavalent chromium by ferrous iron: a process of chromium isotope fractionation and its relevance to natural environments. *Chem. Geol.* **285**, 157–166.
- Ellis A. S., Johnson T. M. and Bullen T. D. (2002) Cr isotopes and the fate of hexavalent chromium in the environment. *Science* **295**, 2060–2062.
- Ellis A. S., Johnson T. M. and Bullen T. D. (2004) Using chromium stable isotope ratios to quantify Cr(VI) reduction: lack of sorption effects. *Environ. Sci. Technol.* **38**, 3604–3607.
- Elovitz M. S. and Fish W. (1994) Redox interactions of Cr(VI) and substituted phenols – kinetic investigation. *Environ. Sci. Technol.* **28**, 2161–2169.
- Elovitz M. S. and Fish W. (1995) Redox interactions of Cr(VI) and substituted phenols – products and mechanism. *Environ. Sci. Technol.* **29**, 1933–1943.
- Espenson J. H. (1970) Rate studies on the primary step of the reduction of Cr(VI) by Iron(II). *J. Am. Chem. Soc.* **92**, 1880–1883.
- Faybishenko B., Hazen T. C., Long P. E., Brodie E. L., Conrad M. E., Hubbard S. S., Christensen J. N., Joyner D., Borglin S. E., Chakraborty R., Williams K. H., Peterson J. E., Chen J. S., Brown S. T., Tokunaga T. K., Wan J. M., Firestone M., Newcomer D. R., Resch C. T., Cantrell K. J., Willett A. and Koenigsberg S. (2008) In situ long-term reductive bioimmobilization of Cr(VI) in groundwater using hydrogen release compound. *Environ. Sci. Technol.* **42**, 8478–8485.

- Frei R., Gaucher C., Poulton S. W. and Canfield D. E. (2009) Fluctuations in Precambrian atmospheric oxygenation recorded by chromium isotopes. *Nature* **461**, 250–253.
- Fruchter J. (2002) In situ treatment of chromium-contaminated groundwater. *Environ. Sci. Technol.* **36**, 464A–472A.
- Gao Y. J., Ma T., Ling W. L., Liu C. F. and Li L. (2010) Analytical method of Cr stable isotope and its application to water pollution survey. *Chin. Sci. Bull.* **55**, 664–669.
- Izbicki J. A., Ball J. W., Bullen T. D. and Sutley S. J. (2008) Chromium, chromium isotopes and selected trace elements, western Mojave Desert, USA. *Appl. Geochem.* **23**, 1325–1352.
- Izbicki J. A., Bullen T. D., Martin P. and Schroth P. (2012) Delta chromium-53/52 isotopic composition of native and contaminated groundwater, Mojave Desert, USA. *Appl. Geochem.* **27**, 841–853.
- Johnson C. A., Sigg L. and Lindauer U. (1992) The chromium cycle in a seasonally anoxic lake. *Limnol. Oceanogr.* **37**, 315–321.
- Johnson C. M. and Beard B. L. (1999) Correction of instrumentally produced mass fractionation during isotopic analysis of Fe by thermal ionization mass spectrometry. *Int. J. Mass Spectrom.* **193**, 87–99.
- Johnson T. M. and Bullen T. D. (2004) Mass-dependent fractionation of selenium and chromium isotopes in low-temperature environments. In *Rev. Mineral Geochem.* (eds. C. M. Johnson, B. L. Beard and F. Albarede). Mineral Society of America, Washington, DC, pp. 289–317.
- Lovley D. R. (1993) Dissimilatory metal reduction. *Annu. Rev. Microbiol.* **47**, 263–290.
- Oze C., Bird D. K. and Fendorf S. (2007) Genesis of hexavalent chromium from natural sources in soil and groundwater. *Proc. Natl. Acad. Sci. USA* **104**, 6544–6549.
- Palmer, C. D. and Puls, R. W. (1994) Natural attenuation of hexavalent chromium in ground water and soils. EPA Ground Water Issue Paper EPA/540/S-94/505, EPA Ground Water Issue Paper EPA/540/S-94/505. US EPA, Washington, p. 12.
- Palmer C. D. and Wittbrodt P. R. (1991) Processes affecting the remediation of chromium-contaminated sites. *Environ. Health Persp.* **92**, 25–40.
- Pettine M. (2000) Redox processes of chromium in sea water. In *Chemical processes in marine environments* (eds. A. Gianguzza, E. Pelizzetti and S. Sammartano). Springer, Berlin, pp. 281–296.
- Pettine M., D'Ottone L., Campanella L., Millero F. J. and Passino R. (1998) The reduction of chromium (VI) by iron (II) in aqueous solutions. *Geochim. Cosmochim. Acta* **62**, 1509–1519.
- Proctor, D. M., Harris, M. A. and Finley, B. L. (eds.) (2000) Chromium in soil: perspectives in chemistry, health, and environmental regulation. *J. Soil Contam.* **6**, 557–797.
- Raddatz A. L., Johnson T. M. and McLing T. L. (2010) Cr stable isotopes in snake river plain aquifer groundwater: evidence for natural reduction of dissolved Cr(VI). *Environ. Sci. Technol.* **45**, 502–507.
- Rees C. E. (1973) A steady-state model for sulphur isotope fractionation in bacterial reduction processes. *Geochim. Cosmochim. Acta* **37**, 1141–1162.
- Refait Ph. and Génin J.-M. R. (1994) The transformation of chloride-containing green rust one into sulphated green rust two by oxidation in mixed Cl^- and SO_4^{2-} aqueous media. *Corros. Sci.* **36**, 55–65.
- Schauble E., Rossman G. R. and Taylor H. P. (2004) Theoretical estimates of equilibrium chromium-isotope fractionations. *Chem. Geol.* **205**, 99–114.
- Schoenberg R., Zink S., Staubwasser M. and von Blanckenburg F. (2008) The stable Cr isotope inventory of solid Earth reservoirs determined by double spike MC-ICP-MS. *Chem. Geol.* **249**, 294–306.
- Scott K. M., Lu X., Cavanaugh C. M. and Liu J. S. (2004) Optimal methods for estimating kinetic isotope effects from different forms of the Rayleigh distillation equation. *Geochim. Cosmochim. Acta* **68**, 433–442.
- Sedlak D. L. and Chan P. G. (1997) Reduction of hexavalent chromium by ferrous iron. *Geochim. Cosmochim. Acta* **61**, 2185–2192.
- Sikora E. R., Johnson T. M. and Bullen T. D. (2008) Microbial mass-dependent fractionation of chromium isotopes. *Geochim. Cosmochim. Acta* **72**, 3631–3641.
- US Department of Health (2000) Toxicological Profile for Chromium. US Department of Health and Human Services, Atlanta.
- Viollier E., Inglett P. W., Hunter K., Roychoudhury A. N. and Van Cappellen P. (2000) The ferrozine method revisited: Fe(II)Fe(III) determination in natural waters. *Appl. Geochem.* **15**, 785–790.
- Wang, X. and Johnson, T. M. (2011) Interpretation of chromium isotopic data: exchange kinetics and fractionation factors between Cr(III) and Cr(VI), Abstract H21A-1048, 2011 Fall Meeting, AGU, San Francisco, CA, 5–9 December.
- Wanner C., Eggenberger U., Kurz D., Zink S. and Mader U. (2012) A chromate-contaminated site in southern Switzerland – Part 1: site characterization and the use of Cr isotopes to delineate fate and transport. *Appl. Geochem.* **27**, 644–654.
- Westheimer F. H. (1949) The mechanisms of chromic acid oxidations. *Chem. Rev.* **45**, 419–451.
- Weyer S. and Schwieters J. B. (2003) High precision Fe isotope measurements with high mass resolution MC-ICP-MS. *Int. J. Mass Spectrom. Ion Processes* **226**, 355–368.
- Wittbrodt P. R. and Palmer C. D. (1996) Effect of temperature, ionic strength, background electrolytes, and Fe(III) on reduction of hexavalent chromium by soil humic substances. *Environ. Sci. Technol.* **30**, 2470–2477.
- Zink S., Schoenberg R. and Staubwasser M. (2010) Isotopic fractionation and reaction kinetics between Cr(III) and Cr(VI) in aqueous media. *Geochim. Cosmochim. Acta* **74**, 5729–5745.

Associate editor: Clark M. Johnson